Fabrication and Optimal Strain Sensor Placement in an Instrumented Disk Drive Suspension for Vibration Suppression

Kenn Oldham, Stanley Kon
Computer Mechanics Laboratory (CML)
University of California at Berkeley, CA
94720-1740

`oldham, kon@me.berkeley.edu`

Roberto Horowitz
Professor of Mechanical Engineering
University of California at Berkeley, CA
94720-1740

`horowitz@me.berkeley.edu`

Abstract— Instrumenting a disk drive suspension with vibration sensing strain gages can enhance vibration suppression in hard disk drives, provided that the gages are properly located and are sufficiently sensitive. The cost function of an optimal LQG controller with Kalman filter is proposed as an objective function for determining the optimal location and orientation of displacement sensors on a flexible structure, such as the placement of strain gages on a disk drive suspension. Analytical bounds are derived for the Kalman filter Riccati equation in a modal system with large sensor noise. These bounds produce analytical approximations that reduce the computational complexity of the LQG optimization approach with cheap control. Results are applied to a prototype disk drive suspension to identify sensor positions and sensor requirements. Methods of installing strain gages on steel at precise locations are briefly discussed.

I. INTRODUCTION

Increasing data storage densities in computer hard disk drives require positioning drives' read-write heads over ever-smaller data bits. As the industry targets bit densities of 1 terabit per square inch, airflow induced vibration of the mechanical servo assembly becomes a major obstacle to attaining the necessary servo precision. In particular, excitation of vibration modes in the e-block and suspension upon which the head and air bearing are mounted will cause significant off-track error during tracking operations.

One method of improving servo capabilities to overcome these problems is to incorporate a second actuator into the servo system to increase servo bandwidth. Currently, disk drives rely on a single large voice-coil motor for actuation (see Fig. Ia and Ib). Proposed dual-stage configurations include actuated suspensions (Fig. 2a), with a microactuator built into the suspension itself, and actuated sliders (Fig. 2b) and heads, with smaller microactuators installed underneath or inside the slider, beyond the vibrating region.

Several researchers have examined the use of additional sensors within a disk drive to better detect and reject vibration disturbances [1] [2] [3]. Adding sensors to the disk drive permits acquisition of vibration information at a higher sampling rate and closer to the point of disturbance than is possible from position error signals taken from the disk itself. This information may be fed back to the VCM or actuated ssuspension or fed forward to actuated sliders and heads (Fig. 2). Micro-scale processing techniques allow precise installation of vibration sensors at locations with
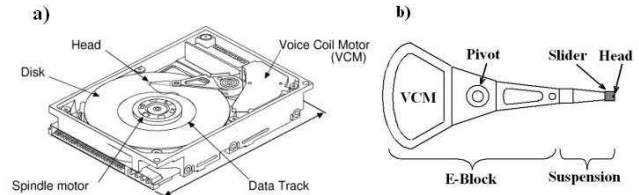

Fig. 1. (a) Conventional disk drive configuration; (b) Conventional disk drive servo assembly
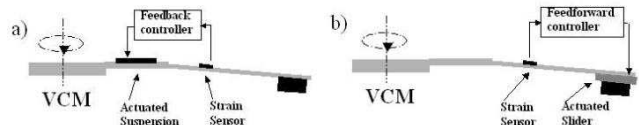

Fig. 2. Dual-stage disk drive servo configurations

maximal vibration information. Meanwhile, certain semiconductor and thin film processing techniques produce very high sensitivity gages, and may potentially be integrated into suspension fabrication and assembly.

In designing a strain gage for vibration detection on a disk drive suspension, it is important to place the gage in a location that provides the maximum amount of useful information to the servo system controller. Not only should a strong signal be available, but it should detect any vibration modes that could contribute to off-track error of the read-write head. However, vibration modes that do not cause off-track error should be avoided by the sensor, as the signal from these modes will unnecessarily excite the controller.

In general terms, finding optimal strain gage locations is a problem of optimal placement of an arbitrary number of displacement sensors on a flexible structure. Hac and Liu [4] applied an observability criteria to this problem, which was adapted to disk drives by Banther, et al. [5] and Gross [6]. Several researchers have proposed using some objective function based on Kalman filter results [7] [8] and Kondoh et al. [9] incorporated controller structure by minimizing the quadratic cost function in standard linear-quadratic-gaussian (LQG) optimal control. The solution of the LQG problem provides an optimal result in terms of the H2 norm of the system, but the approach is computationally intensive and requires knowledge of the stochastic properties

of the system.

In this paper, we optimize sensor locations on a disk drive suspension according to the cost function of the standard LQG problem, but present numerical approximations of the Riccati equation solutions to simplify computational complexity and relax requirements on knowledge about the stochastic system. We compare the choices of optimal sensor location according to exact and approximate methods and comment on methods for fabricating the optimized sensors.

II. PROBLEM DESCRIPTION AND THEORY

A. System Model

The disk drive servo system described here consists of the flexible suspension with inputs from the voice coil motor (VCM) and airflow disturbances, plus an actuated-slider microactuator at the tip of the suspension. The motion of a flexible structure can be written as the summation of modal contributions. For instance, off-track displacement, z, of the read-write head may be written as

$$z = \sum_{i=1}^{n} d_i \nu_i + x_{MA} \tag{1}$$

where ν_i is a modal coordinate for mode i, d_i is the displacement at the tip of the suspension in the modal coordinate for mode shape i, x_{MA} is the displacement of the microactuator relative to the tip of the suspension, and n is the number of modes considered.

Similarly, strain gage measurements from this system are

$$y_k = \sum_{i=1}^{n} c_{ki} \nu_i \qquad c_{ki} = K_{sense} c'_{ki} \tag{2}$$

where y_k is the strain gage output voltage and c_{ki} is the magnitude of strain, ϵ at the sensor location resulting from mode i, c'_{ki}, times the sensor gain, K_{sense} in V/ϵ.

The modal dynamics are driven both by the VCM and disturbances:

$$\ddot{\nu}_i + 2\xi_i \omega_i \dot{\nu}_i + \omega_i^2 \nu_i = \sum_{k=1}^{l} b_{ik} \omega_i^2 w_k + \omega_i^2 u_{VCM} \tag{3}$$

Here, the dynamics of each mode are described by its natural frequency, ω_i, and damping ration, ξ_i. The modal coordinates are normalized to ω_i^2 times the VCM input for convenience in later manipulation. The b_{ik} coefficients adjust disturbance k for its influence relative to the VCM on mode i, due to differing location and frequency weighting.

The microactuator dynamics have a similar description,

$$\ddot{x}_{MA} + 2\xi_{MA}\omega_{MA}\dot{x}_{MA} + \omega_{MA}^2 x_{MA} = K_{MA} u_{MA} \tag{4}$$

with ω_{MA} and ξ_{MA} the natural frequency and damping ratio of the microactuator, and K_{MA} the microactuator gain.

In state space, the system may be described in the form

$$\dot{x} = Ax + Bu + B_w w \qquad y = Cx + v \qquad z = Dx \tag{5}$$

$$E[ww^T] = \mathrm{w} I_{l \times l} \qquad E[vv^T] = \mathrm{v} I_{r \times r} \tag{6}$$

Again, $z \in \mathbb{R}$ is off-track error at the slider and $y \in \mathbb{R}^{r+1}$ is output from r strain gages plus an additional measurement of relative position error signal (RPES) measured by the microactuator. The inputs are l white disturbances in $w \in \mathbb{R}^l$ with spectral density w and two actuated inputs, from the VCM and microactuator, included in $u \in \mathbb{R}^2$. Sensor noise is $v \in \mathbb{R}^r$, white with spectral density v. Experimental studies have verified that airflow excitation has broadband frequency spectrum and can be accurately modelled by zero-mean input white noise [10] [11].

The state vector $x \in \mathbb{R}^{2n+2}$ consist of the modal and microactuator coordinate displacements and normalized velocities,

$$x_{2i-1} = \nu_i \qquad x_{2i} = \frac{\dot{\nu}_i}{\omega_i} \tag{7}$$

$$x_{2N+1} = x_{MA} \qquad x_{2N+2} = \frac{\dot{x}_{MA}}{\omega_{MA}} \tag{8}$$

The state matrices are

$$A = \mathrm{diag} \begin{pmatrix} A_1 & \cdots & A_{n_{MA}} \end{pmatrix} \tag{9}$$

$$A_i = \begin{bmatrix} 0 & \omega_i \\ -\omega_i & -2\xi_i\omega_i \end{bmatrix} \qquad A_{MA} = \begin{bmatrix} 0 & \omega_{MA} \\ -\omega_{MA} & -2\xi_{MA}\omega_{MA} \end{bmatrix} \tag{10}$$

$$B = \begin{bmatrix} 0 & 0 & \cdots & 0 & 0 & 0 & K_{MA}\omega_{MA} \\ 0 & \omega_1 & \cdots & 0 & \omega_n & 0 & 0 \end{bmatrix}^T \tag{11}$$

$$B_w = \begin{bmatrix} 0 & b_{11}\omega_1 & \cdots & 0 & b_{n1}\omega_n & 0 & 0 \\ \vdots & \vdots & & \vdots & \vdots & \vdots & \vdots \\ 0 & b_{1l}\omega_1 & \cdots & 0 & b_{nl}\omega_n & 0 & 0 \end{bmatrix}^T \tag{12}$$

$$C(\Phi) = \begin{bmatrix} c_{11}(\Phi_1) & 0 & \cdots & c_{1n}(\Phi_1) & 0 & 0 & 0 \\ \vdots & \vdots & & \vdots & \vdots & \vdots & \vdots \\ c_{r1}(\Phi_r) & 0 & \cdots & c_{rn}(\Phi_r) & 0 & 0 & 0 \\ 0 & 0 & \cdots & 0 & 0 & c_{es} & 0 \end{bmatrix} \tag{13}$$

$$D = \begin{bmatrix} d_1 & 0 & \cdots & d_n & 0 & 1 & 0 \end{bmatrix} \tag{14}$$

b_{ij} and d_i are defined as before, while $c_{ij}(\Phi_j)$ is the strain from mode j measured at strain gage i, written explicitly as function of the location and orientation, Φ_i, of the sensor. c_{es} is the RPES signal gain from the microactuator.

B. Optimization Theory

Our objective is to choose a sensor location and orientation that minimizes off-track error of the closed-loop system. We choose to minimize the H2 norm of the system when implementing the optimal linear quadratic gaussian, or LQG, controller and filter.

$$\min_{\Phi} J_{H2} = \min_{\Phi} \left\{ \min_{K,F(\Phi)} E \left[z^T z + u^T R u \right] \right\} \tag{15}$$

with K the optimal linear, stationary controller, $F(\Phi)$ the optimal linear, stationary filter for a given $C(\Phi)$, and R a weighting function on the inputs. Vector Φ includes all coordinates and orientations of sensors that may be varied during optimization.

K and F are obtained by solving Riccati equations. The linear controller, K, for this system is not dependant on sensor location:

$$u = -K\hat{x} \tag{16}$$

$$K = R^{-1}B^T P \tag{17}$$

$$A^T P + PA - PBR^{-1}B^T P + D^T D = 0 \tag{18}$$

The optimal linear filter, F, is a Kalman filter and does depend on sensor location

$$\dot{\hat{x}} = A\hat{x} + Bu + MC(\Phi)^T \mathrm{v}^{-1}[\hat{y} - C(\Phi)\hat{x}] \tag{19}$$

$$F = MC(\Phi)^T \mathrm{v}^{-1} \tag{20}$$

$$AM + MA^T - MC(\Phi)^T \mathrm{v}^{-1}C(\Phi)M + B_w \mathrm{w} B_w^T = 0 \tag{21}$$

The value of the objective function with this controller and filter is

$$J_{H2} = tr\left[PF\mathrm{v}F^T + MD^T D\right]. \tag{22}$$

The drawbacks of this optimization method are requirements on knowledge about the system and computational complexity. Reasonable results require reliable estimates of disturbance and noise magnitudes. Even when this information is available, solving the Riccati equation at many locations requires a large amount of computation time. In the following section, we describe an approximation for the Riccati equation in a system described by the modal components described previously.

An alternative to LQG optimization is to optimize some measure of the observability of the system. The observability gramian, Q, for an asymptotically stable state space system satisfies

$$A^T Q + QA + C(\Phi)^T C(\Phi) = 0. \tag{23}$$

The eigenvalues of the observability gramian are a measure of the energy from each mode for a given sensor placement, and can thus be used as a basis for locating sensors. Various objective functions based on eigenvalues of the observability gramian have been proposed, as in [5] and [4]. However, as will be discussed later, observability approaches may neglect the relative importance of the modes in causing off-track error, and not necessarily provide the best signal in a closed-loop system.

C. Approximate Riccati Solution

While an exact analytical solution to the Riccati equation exists, it requires a large number of calculations and can make optimization impractical, especially for a large numbers of variables. A 2n-eigenvalue problem must be solved to obtain the estimation error covariance matrix M at each location Φ. Observability-based approaches are also relatively complex, requiring solution of an n-eigenvalue problem. This makes sensor optimization difficult for systems with large numbers of modes or many potential sensor locations.

To mitigate this problem, we have derived a set of approximations for error covariance matrix M. For a system with the state space form above, bounds may be placed on certain terms of matrix M, including all those which appear in objective function (22). Under certain conditions, these bounds approximate the values of the diagonal terms in M and show them to be much larger than the off-diagonal terms. The full derivation of the approximations is included the Berkeley CML Report by this title [13].

The chief approximation result is that, for a system of the type described by equations (1- 3), if for all i and j,

1) Modes are widely spaced:

$$|\omega_i - \omega_j| \gg 0 \tag{24}$$

2) Sensor noise is large relative to other parameters:

$$|c_{ji}|\left(\sum_{k=1}^{l}|b_{ik}|\right)\frac{\mathrm{w}}{\mathrm{v}} \ll 1 \tag{25}$$

then, for all i, in an undamped system

$$m_{2i-1,2i-1} \approx \frac{\sqrt{\sum_{p=1}^{l}b_{ip}^2}\,\omega_i\sqrt{\mathrm{wv}}}{\sqrt{\sum_{k=1}^{r}c_{ki}^2}} \tag{26}$$

and in a lightly damped system

$$m_{2i-1,2i-1} \approx \frac{-4\xi_i\omega_i + \sqrt{(4\xi_i\omega_i)^2 + \frac{4\omega_i^2 \mathrm{w}}{\mathrm{v}}\left(\sum_{k=1}^{r}c_{ki}^2\right)\left(\sum_{p=1}^{l}b_{ip}^2\right)}}{\frac{2}{\mathrm{v}}\sum_{k=1}^{r}c_{ki}^2} \tag{27}$$

.

Furthermore, in both cases, for all $i \neq j$,

$$m_{2i-1,2i-1} \gg m_{2i-1,2j-1}. \tag{28}$$

Since the range of motion of both the VCM and microactuator is very large relative to suspension vibration, we solve the above equations for the case of cheap control, $R \to 0$. From loop transfer recovery (LTR) results [15], in this situation $P \to 0$ and

$$J_{H2} \approx \sum_{i=1}^{n} d_i^2 m_{2i-1,2i-1} \tag{29}$$

with m from (26) or (27).

If non-cheap control were required, the cost would be

$$J_{H2} \approx \sum_{i=1}^{n} d_i^2 m_{2i-1,2i-1} +$$

$$\sum_{i=1}^{n}\sum_{j=1}^{n} p_{2i-1,2j-1} m_{2i-1,2i-1} m_{2j-1,2j-1}\left(\sum_{k=1}^{r} c_{ki}c_{kj}\right) \tag{30}$$

Here, p_{ij} is the (i,j)th term of the stationary Riccati solution P from (18). Notice that P need only be solved for once, since it does not depend on sensor location. Analogous results exist for a discrete time system derived from the continuous time model described above.

Approximating the objective function in this manner has several advantages. Its main effect is that it greatly simplifies

the computation of the objective function. It reduces the problem of solving for n eigenvalues to a straightforward algebraic computation. In our tests, this reduced computation time by a factor of 20. The relative computational benefit in the case of non-cheap control is the same. This is especially important for a system with many modes or sensor location variables. The approximation allows the optimal solution to be found easily for varying system parameters where a exact solution would be highly impractical. However, the approximation also gives insight into physical trade-offs between parameters of the system, and reduces the amount of knowledge about the system needed beforehand.

First, we comment on the conditions under which the approximation holds. Widely-spaced modes are a common requirement for simple analysis of modal systems. More interesting is the second condition, (25), which indicates that the approximation applies to systems with large sensor noise. In fact, it seems to imply that the signal from the sensors will be below the noise floor of the system, but the addition of multiple modes and the presence of resonant peaks can raise the signal well above the noise floor while (25) remains satisfied. Furthermore, many of the bounds used to derive the approximation are loose, so that the approximation may be reasonable even for smaller noise levels. The approximation should be checked against the exact solution for several test cases if this is attempted.

When the approximation does perform well, the relative significance of the parameters in the system model is visible, which can be useful for design and interpretation; a criticism of the use of Kalman filter methods for optimizing sensor locations is lack of a physical interpretation of the result. The best sensor locations will have large strains (large c_{ki} coefficients), as one would expect. However, in a choosing between strain contributions from different modes when there is a trade-off, a more optimal location will emphasize the mode with a larger contribution to off-track error, as computed from the sum of input coefficients to that mode, the b_{ip}'s, and the modal displacement coefficient at the slider, d_i. In non-cheap control, the cost of controlling that mode is added in, while including damping in the system diminishes the difference between modal contributions.

We can compare our proposed method to the observability methods. For a lightly-damped system, the eigenvalues of the observability grammian can be approximated as

$$\lambda_{2i-1}, \lambda_{2i} \approx \frac{\sum_{k=1}^{r} c_{ki}^2}{4\xi_i\omega_i}. \tag{31}$$

Maximizing the minimum eigenvalue is equivalent to minimizing the maximum inverse eigenvalue, or,

$$J_{opt} = \min_{C(\Phi)} \left[\max_i \left\{ \frac{4\xi_i\omega_i}{\sum_{k=1}^{r} c_{ki}^2} \right\} \right]. \tag{32}$$

The value to be minimized in the observability case is qualitatively similar to the LQG filter result, but the relative importance of each mode to off-track error is lacking. As a result, the observability approach will locate sensors so as to best detect modes with small strain contributions, ignoring more easily detected modes. If one of these modes causes proportionally larger off-track error than strain signal, it may be lost by the sensor at levels that cause significant off-track error. One solution, used in [6], is to weight the eigenvalues by their modal contribution to off-track error. This tends to give close agreement with LQG results, though it still neglects input coefficients and requires more computation.

Finally, the approximate solution shows that, for a noisy system, the optimal sensor location is independent of the exact noise and disturbance strength. Each of the diagonal terms in M is multiplied by the same $\sqrt{\text{wv}}$ constant. This means that only enough knowledge about the stochastic properties of the system to validate the approximate solution is required. The exact noise and disturbance levels need not be known prior to design of the system.

III. OPTIMIZATION RESULTS FOR DISK DRIVE SUSPENSION

A. Optimization Implementation

A commercial suspension was modelled in ANSYS for finite element analysis of vibration modes. A modal analysis was performed to identify the natural frequencies of vibration, followed by a harmonic analysis near those frequencies to obtain the frequency response of the structure. The analysis provided transfer functions from VCM input to off-track displacement and to x-normal, y-normal, and xy-shear components of strain at any model element.

$$\frac{Z(s)}{U(s)} = \sum_{i=1}^{n} \frac{d_i\omega_i}{s^2 + 2\xi_i\omega_i s + \omega_i^2} \tag{33}$$

$$\frac{Y_k(s)}{U(s)} = \sum_{i=1}^{n} \frac{c'_{ki}\omega_i}{s^2 + 2\xi_i\omega_i s + \omega_i^2} \tag{34}$$

Here, $U(s)$ is the VCM input in the frequency domain, $Z(s)$ the frequency response of off-track error, and $Y_k(s)$ the component of strain at sensor k in any single strain direction. Damping ratios, modal weights, and gains for d_i and c'_{ki} were obtained by the circle fit modal identification method.

The x-, y-, and xy- components of strain at each element were projected to a voltage output for an arbitrary strain gage orientation θ using Mohr's equation and the estimated gage sensitivity K_{sense},

$$C = K_{sense} \left[\begin{array}{ccc} \frac{1+\cos 2\theta}{2} & \frac{1-\cos 2\theta}{2} & \frac{\sin 2\theta}{2} \end{array} \right] \left[\begin{array}{c} C_{\text{x}} \\ C_{\text{y}} \\ C_{\text{xy}} \end{array} \right], \tag{35}$$

where C_{x}, C_{y}, and C_{xy} are the sensor output coefficients for the three strain components.

Stochastic parameters of the system (w,v) are estimated from strain gain models and experimental measurements of suspension vibration in other disk drives at $w = 1 \times 10^{-7}$ mN^2 and $v = 1 \times 10^{-15}$ V^2. We use a single

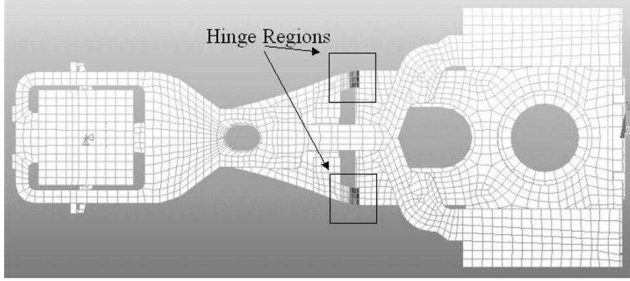Fig. 3.   Ansys model of 3430 suspension

Fig. 4.   Optimal sensor locations (dark to light), cheap control $R \to 0$

disturbance and set input coefficients b_{11} to b_{41} equal to one, and reduce b_{51} and b_{61} to 0.5 and 0.1, respectively to reflect lower windage measurements at frequencies above 10 kHz. A more accurate model would include adjustments to all b_i's to match both spatial and frequency domain properties of the input disturbance, but this information is not well known. Sensor gain, K_{sense}, from our preliminary fabrication studies is estimated at 60. For our non-cheap control example, we set $R = 10^{-8}$, which gives approximately equal contributions to total cost from off-track error and control effort.

We have set up this problem as a dual-stage system, but because our system model does not include a disturbance to the microactuator, the microactuator mode is not in the correct form for our approximation. Fortunately, with the microactuator largely decoupled from the rest of the system, its effect on the cost function is very small. For $R \le 2 \times 10^{-8}$, neglecting the microactuator gives less than a 1% change in total cost. In reality, there may be some coupling between suspension vibration and microactuator displacement and correlation between disturbances to the suspension and microactuator. This could provide additional information about suspension vibration and thus influence sensor selection, but we choose not to assume that this information will be available.

B. Location Optimization Results

We evaluated the LQG cost function at 100 high-strain elements in the hinge region of the suspension at sensor orientations from 0 to 180 degrees. The cost function was evaluated for both the exact solution for the Kalman filter Riccati equation and for the approximate solution discussed above. Fig. 3 shows the full ANSYS model of the suspension with the hinge regions highlighted. Fig. 4a and 4b show the 20 best elements for strain gage installation using both evaluations. Both the exact solution and the approximation identify element 1346 as optimal, with the strain gage oriented at $11°$ for the exact solution and $10°$ for the approximation. For non-cheap control, the same optimal element is chosen, as shown in Fig. 5, but the optimal angle is reduced to $10°$ in the exact solution, and the distribution of good elements is shifted slightly up the suspension.

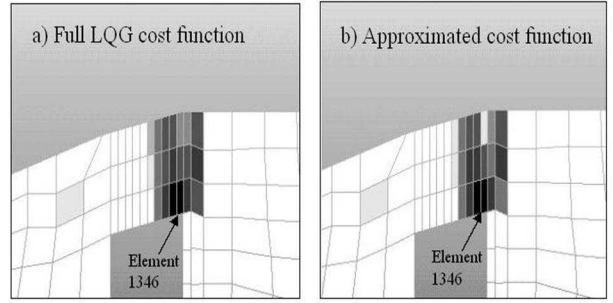The dynamic response from disturbance to sensor output and off-track error is shown in Fig. 6. The best sensor location will have both a high level of strain and a large ratio of strain to off-track response at each mode. This results in a position that approximately matches the importance of modes at the sensor to their importance to off-track error at the slider. For this sensor location, the most difficult mode to detect is mode 5, a torsion mode, for which a disturbance producing one nanometer off-track displacement would produce 56 nanostrain at the sensor.

It is also clear from Fig. 4 that the approximate solution to the LQG cost function gives results that are very similar to the exact solution. This agreement can also be seen a individual sensor locations as a function of orientation. Fig. 7 plots the cost function as a function of angle for optimal element 1346. Both methods show undesirable orientations at 75 and 122 degrees, and close agreement elsewhere.

The approximation we have developed is applicable to this situation because the strain in the system is very small, ranging from 10 to 100s of nanostrain for the level of disturbance anticipated. This results in very small c_{ki} coefficients that help satisfy (25). The largest value for a quantity in (25) is 0.16, large enough to cause some discrepancy between exact and approximate Riccati solutions, but still giving generally good agreement. Table I is an example of this: while the error between estimated and exact diagonal coefficients is as high as 33%, this is a small discrepancy for a set of diagonal terms of M that range over 3 orders of magnitude. Additionally and as expected, the largest off-diagonal term is much smaller, at $m_{7.9} = 1.7 \times 10^{-8}$.
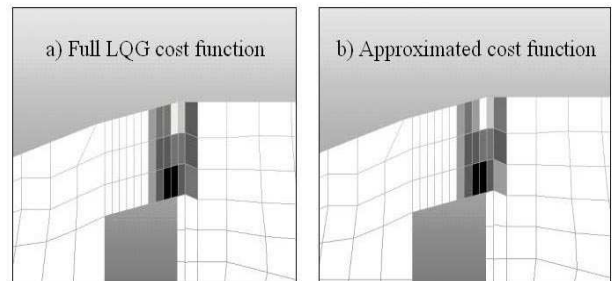

Fig. 5.   Optimal sensor locations (dark to light), $R = 10^{-8}$
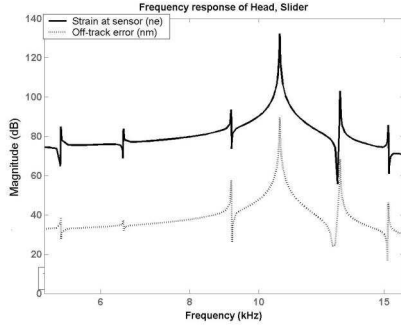
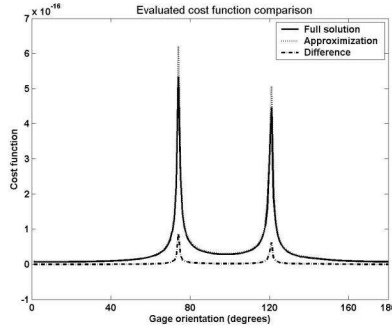Fig. 6. Frequency response of sensors and off-track disturbance

Fig. 7. Cost function by sensor orientation, element 1346

C. Sensor Fabrication

We are currently exploring several methods for installing strain gages at the locations identified by our optimization procedure. The sensors' targeted resolution is 56 nanostrain, corresponding to a maximum of one nanometer displacement from any individual mode based on our optimization results. MEMS-style processing and photolithography permit fabrication of very small sensors at precise locations. Furthermore, highly sensitive materials, such as piezoresistive semiconductors and piezoelectric films are available. However, using these techniques and materials with steel substrates imposes certain constraints on the fabrication procedure. Any treatments to the substrate itself must be performed at low temperatures to avoid altering the suspension's material properties, thus limiting materials available for direct deposition. The finished device must also be robust enough to survive later suspension processing steps, particularly bending the hinge region to set suspension pre-load.

TABLE I

COMPARISON OF EXACT AND APPROXIMATE RICCATI SOLUTION

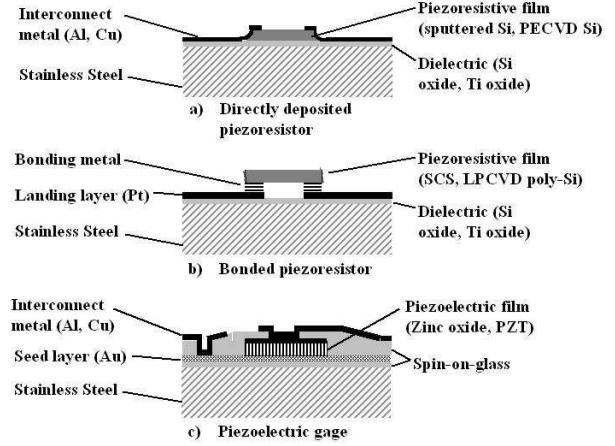| Mode i	ω_i (Hz)	$m_{2i-1,2i-1}$	Approximation	Error
1	5275	1.27	1.38	7.9%
2	6457	1.58	1.78	12.7%
3	9144	1.12	1.49	33.3%
4	10698	0.0271	0.0274	1.1%
5	13002	0.208	0.215	3.5%
6	15197	0.0368	0.0385	4.6%

Fig. 8. Cross-sections of proposed stain gages

TABLE II

PROJECTED PIEZORESISTIVE SENSOR PERFORMANCE

Material	Const-anten	Single crystal Si [16]	p-type poly-Si [17]	n-poly LPCVD poly-Si	αSi:H [18]
Gage factor	2.1	150	30	10	20
S_{bridge} (V/ϵ)	12.6	900	180	60	120
Thickness (μm)	0.5	2.0	2.0	1.0	1.0
Resistivty (Ωcm)	5e-5	0.05	1.0	0.006	1.0
Resistance $(k\Omega)$	0.49	2.5	25	0.3	25
Total noise (μV)	1.1	1.4	3.1	1.1	3.1
Resolution $(n\epsilon)$	91	1.6	17	19	26

Table II compares various piezoresistive materials based on their gage factor, noise, and resolution for a single FEA element-sized 100 μm long by 20 μm wide strain gage and a 5 $nV/\sqrt{Hz}$ electronics noise level. Conventional metal strain gages, such as constanten, are not sensitive enough for the necessary resolution without extremely clean circuitry. Semiconductor films deposited at low temperatures, such as amorphous hydrogenated silicon (αSi:H) tend to be limited by intrinsic thermal noise due to poor conductivity, but, adapted to a steel substrate, may still achieve the necessary resolution. Finally, single-crystal silicon and high-temperature polysilicons project the best performance, but these cannot be deposited directly on steel without violating temperature constraints.

Direct deposition of a piezoresistive material on a steel substrate is the simplest method of fabricating strain gages on steel substrates. The piezoelectric may be patterned directly and a simple metal interconnect added on top, as shown in Fig. 8a. Our initial fabrication tests used sputtered silicon for its simple deposition. A gage factor near 15 was observed, but we have been unable to reduce resistivity below 200 Ω-cm, limiting resolution to approximately 200 nanostrain. The sensors were patterned from highly-doped p-type silicon sputtered on steel coated with a dielectric, plasma-enhanced chemical vapor deposited (PECVD) silicon oxide. Film quality was mainly limited by contamination from the sputtering process, along with low dopant acti-

vation and mobility in the unstructured film. More complex deposition techniques, such as laser-crystallized polysilicon and certain PECVD silicon deposition, may produce more conductive sensors.

To capitalize on the extreme sensitivity of single crystal silicon, we are also constructing sensors to be bonded to steel, using a direct metal-on-metal bonding procedure developed by Microassembly Technologies, Inc. A metal landing layer is patterned on the steel substrate, with landing pads, interconnects, and external bond pads, while sensors are fabricated from the device layer of a silicon-on-insulator wafer. The sensors are undercut in a wet etch, leaving them attached only by thin tethers to the handle wafer. Metal bonding bumps are deposited on the sensors and the two substrates are pressed together, forming a cold weld between bumps and landing pads. Removing the handle wafer breaks the tethers and leaves the sensors on the steel. This sensor's cross-section is shown in Fig. 8b.

An alternative to piezoresistive sensing is to use a piezo-electric film, which may provide an even higher sensitivity than semiconductor materials. The difficulty of this approach is forming a high quality piezoelectric film on a rough steel surface. We have been able to deposit sputtered zinc oxide films with sensitivity as good as one-fifth that of bulk zinc oxide by planarizing the steel surface with spin-on-glass and using a gold seed layer. This sensitivity projects to single nanostrain sensor resolution, but the full processing sequence is noy yet tested. The zinc oxide film must be capped with an etch stop layer, patterned into sensors, and topped with interconnects to external bond pads. Such a sensor is shown in Fig 8c. We are currently testing patterned zinc oxide sensors.

IV. Conclusions and Future Work

In this paper we have examined the design and fabrication of an instrumented disk drive suspension. We proposed the optimization of sensor location based on the cost function of an LQG controller and filter. An approximation for the cost function is derived for low-cost control in a noisy system to reduce computational complexity and gain insight into optimization results. The optimal location for a single strain gage on a sample suspension was identified on the upper inside of the hinge region, with good agreement between exact and approximate optimization methods. We are currently testing strain gage fabrication methods to produce strain gages at optimal locations on steel suspensions.

Future improvements to the instrumented suspension design involve refinement of both sensor optimization and fabrication. The simplifying approximations introduced for the optimization scheme may be used to quickly evaluate multiple sensor schemes. To accommodate more robust controller designs, it will also be useful to adapt the optimization scheme to reject strain sources, such as suspension bending modes, that do not correspond to off-track motion at the read/write head. The final choice of sensor locations and fabrication techniques will be used to assemble a full

instrumented suspension for integration in a dual-stage disk drive servo system.

References

[1] Huang, Y., M. Banther, P. Mathur and W. Messner, Design and analysis of a high bandwidth disk drive servo system using and instrumented suspension, *IEEE/ASME Trans. Mech.*, vol. 4, no. 2, 1999, pp. 196-206.

[2] Huang, F.Y., T. Semba, W. Imaino and F. Lee, Active damping in hdd actuator, *IEEE Trans. Mag.*, vol. 37, no. 2, 2001, pp. 847-849.

[3] Li, Y., R. Horowitz and R. Evans, Vibration control of PZT actuated suspension dual-stage servo system using a PZT sensor, *IEEE Trans. Mag.*, vol. 30, no. 2, 2003, pp. 932-936.

[4] Hac, A. and L. Liu, Sensor and actuator location in motion control of flexible structures, *J. Sound and Vibration*, vol. 167, no. 2, 1993, pp 239-261.

[5] Banther, M., Y. Huang and W. Messner, "Optimal strain gage placement for an instrumented disk drive suspension", *Proc. American Control Conf.*, Philadelphia, PA, 1998, pp. 3023-3027.

[6] Gross, H., University of California, Berkeley, dissertation, Berkeley, CA, 1988.

[7] Juang, J.N. and G. Rodriguez, "Formulations and applications of large structure actuator and sensor placements", *Proc. YPI&SU/AIAA Symposium on Dynamics and Control of Large Flexible Spacecraft*, 1979, pp. 247-262.

[8] Hiramoto, K., H. Doki, and G. Obinata, Optimal sensor/actuator placement for vibration control using explicit solution of algebraic Riccati equation. *J. Sound and Vibrataion* Vol. 229, No. 5, 2000, pp.1057-1075.

[9] Kondoh, S., C. Yatomi, and K.Inoue, The positioning of sensors and actuators in the vibration of flexible systems, *JSME Int'l J.*, vol. 33, 1990, pp. 145-152.

[10] Yamaguchi, Y., K. Takahashi, and H. Fujita, Flow induced vibration of magnetic head suspension in hard disk drive. *IEEE Trans. Mag.*, Vol. 22, No. 5, 1986, pp.1022-1024.

[11] Shimizu, H., T. Shimizu, M. Tokuyama, H. Masuda, and S. Nakamura, Numerical simulation of positioning error caused by air-flow-induced vibration of head gimbals assembly in hard disk drive. *IEEE Trans. Mag.*, Vol. 39, No. 2, 2003, pp.806-811.

[12] Shaked, U., Explicit solution to the singular discrete-time stationary linear filtering problem. *IEEE Trans. Automatic Control*, Vol. AC-30, No.1, 1985, pp. 34-47.

[13] Oldham, K., S. Kon, and R. Horowitz, Fabrication and optimal strain sensor placement in an instrumented disk drive suspension for vibration suppression, *Computer Mechanics Laboratory Blue Report*, Nov. 2003.

[14] Yen, J.Y., University of California, Berkeley, dissertation: Identification and control of a computer disk drive actuator, Berkeley, CA, 1988.

[15] Athans, M. A tutorial on the LQG/LTR design method. *Proc. American Controls Conf.*, vol. 2, 1986, pp.1289-1296.

[16] Mason, W.P., *Crystal Properties of Interaction Processes*, Academic Press, New York; 1966.

[17] Obermeier, E. and P. Kopyztynski, Polysilicon as a material for microsensor applications, *Sensors & Actuators A - Physical* Vol. 30 No.1 pp. 149-155.

[18] Spear, W.E. and M. Heintze, The effects of applied and internal strain on the electronic properties of amorphous silicon. *Philosophical Magazine B-Physics of Condensed Matter Structural Electronic Optical & Magnetic Properties*, vol.54, no.5, 1986, pp. 343-58.